Environmental Science
Water Research & Technology

Aerobic Oxidation of Arsenite to Arsenate by Cu(II)-chitosan/O2 in Fenton-like Reaction, a XANES Investigation

Journal:	*Environmental Science: Water Research & Technology*
Manuscript ID	EW-ART-04-2020-000326.R1
Article Type:	Paper

Water impact statement:

Fenton(-like) reactions are widely used in water treatment applications to oxidize and degrade organic pollutants; however, oxidation of inorganic contaminants via Fenton(-like) processes has been much less frequently studied. In this study, As(III) is used as a probe molecule to demonstrate the successful oxidation of As(III) to As(V) by Cu(II)-chitosan via a Fenton-like reaction.

Aerobic Oxidation of Arsenite to Arsenate by Cu(II)-chitosan/O_2 in Fenton-like Reaction, a XANES Investigation

Lauren N. Pincus[a,b], Isabel S. Gonzalez[c], Eli Stavitski[d], Julie B. Zimmerman[a,b,c*]

[a]Yale University, School of Forestry and Environmental Studies, 195 Prospect St., New Haven, CT 06511, United States

[b]Nanosystems Engineering Research Center for Nanotechnology-Enabled Water Treatment (NEWT), Yale University, New Haven, CT 06511

[c]Yale University, Department of Chemical and Environmental Engineering, 17 Hillhouse Ave, New Haven, CT 06511, United States

[d]National Synchrotron Light Source II, Brookhaven National Laboratory, Upton, NY 11973, USA

*Corresponding author. Yale University, Department of Chemical and Environmental Engineering, United States, Telephone: +1 (203) 432-9703, julie.zimmerman@yale.edu

Abstract

Oxidation of inorganic molecules (e.g., arsenite (As(III)) to arsenate (As(V))) by Cu(II)-chitosan in the presence of dissolved oxygen is examined to elucidate the ability and mechanism of Cu(II)-chitosan and Cu(II)-n-TiO_2-chitosan participation in Fenton-like reactions. To form the Cu(II)-chitosan complex, Cu(II) binds with the amine groups of the chitosan backbone resulting in a Cu(II)-complex with cationic behavior. Arsenic is then adsorbed to the copper binding site through a combination of Lewis acid-base coordinate bonding and electrostatics. As K-edge XANES indicate that arsenite is fully oxidized to arsenate when adsorbed to a Cu(II)-chitosan complex in the dark without introduction of a photo- or chemical-oxidant. The oxidation of arsenite by this complex is strongly controlled by the presence of dissolved oxygen as suggested by linear combination fitting where the %As(V) bound decreases from 100% ± 0.0% to 60.2 ± 0.1% upon removal of dissolved oxygen via the freeze pump thaw method. Cu K-edge XANES indicate that Cu(II) acts as a catalyst rather than a reactant, as it remains present as Cu(II) after As oxidation in each system condition examined. For Cu(II)-n-TiO_2-chitosan, the amount of As(III) oxidized to As(V) is strongly controlled by the loading of Cu(II), with a higher loading of Cu(II) leading to more As(III) oxidized and bound on the surface of the adsorbent as As(V).

As(III) removal by both Cu(II)-chitosan and Cu(II)-nTiO_2-chitosan are significantly improved due to the Fenton-like oxidation of As(III) to As(V). For Cu(II)-n-TiO_2-chitosan, higher loadings of Cu(II) relative to n-TiO_2 lead to greater improvement of As(III) removal performance in oxic vs anoxic conditions.

Key words: arsenic, adsorption, Cu(II), Fenton-like, oxidation; chitosan

1. Introduction

Fenton and Fenton-like reactions have been widely used within advanced oxidation processes (AOPs) as an effective means to oxidize organic contaminants with high chemical stability and/or low biodegradability, converting them into less toxic or more easily biodegradable molecules.[1,2] Iron catalyzed Fenton reactions can also be utilized to oxidize or reduce inorganic contaminants, (e.g., As(III); Cr(VI)) into their less toxic and more easily removed oxidation states.[3,4] Benefits of using Fenton-type chemistry include short reaction times, lack of waste generation, and the use of relatively inexpensive and environmentally benign materials (e.g., hydrogen peroxide) and low-cost metals, (e.g., iron and copper).[2,5] In a traditional Fenton reaction, Fe(II) first reacts with H_2O_2 to form a Fe(II)-peroxide complex.[6] This complex then decomposes into reactive oxidants, either hydroxyl radicals or Fe(IV)[6] that can oxidize various compounds.

Less frequently studied than traditional iron catalyzed Fenton reactions are Fenton-like reactions involving other transition metals such as, Cu(II), which can similarly react with H_2O_2 to form reactive oxidants in the form of hydroxyl radicals and Cu(III). These reactive oxidants are pH dependent with hydroxyl radicals more commonly produced in acidic conditions and Cu(III) in neutral and alkaline conditions.[6,7] Cu(II) catalyzed Fenton-like reactions have been used successfully to oxidize and degrade various organic compounds including acetaminophen,[8] benzoate,[6,7] phenol,[6] and methanol;[6] however, inorganic contaminants, such as arsenic, have not yet been reported to be successfully oxidized via a Cu(II) catalyzed Fenton-like reaction.

Arsenic is a toxic and carcinogenic metalloid that can be released into waters both naturally and anthropogenicly.[9–11] The forms of arsenic predominantly found in aqueous environments are arsenite (As(III)) and arsenate (As(V)).[10] At pH 5-7, As(V) tends to be negatively charged ($H_2AsO_4^-$ and $HAsO_4^{2-}$). In contrast, As(III), the more toxic form of arsenic, is typically

uncharged (H_3AsO_3), making it more difficult to remove.[12,13] Therefore, arsenite is commonly oxidized to arsenate as a pre-treatment step[14–16]. One of the most frequently used techniques is photo-catalysis of As(III) to As(V) by n-TiO_2 in UV light. This oxidation reaction occurs as follows: 1. Superoxide radicals are generated on the surface of n-TiO_2 under UV light react with As(III) to produce As(IV) radicals, 2. Molecular oxygen, hydroxyl radicals, or a trapped hole react with As(IV), oxidizing it to As(V).[15,17] While this method of arsenic oxidation is effective, it can be challenging to incorporate UV light into a flow-through water treatment systems at a reasonable scale.[18]

An alternative technique to photooxidation of As(III) to As(V) is Fenton and Fenton-like reactions using Fe(II) ions and hydrogen peroxide.[6,19,20] However, in the case of Cu(II) Fenton-like reactions, Cu(II) ions and H_2O_2 were unable to oxidize As(III) to As(V) except in high alkalinity conditions, likely due to the low reaction rate.[6] One technique to overcome this barrier that has been reported is the addition of hydroxylamine, a reducing agent, into the Cu(II)/H_2O_2 system which accelerates the rate of Cu(II) reduction, as well as the production of reactive oxidants by Cu(II)/H_2O_2.[6,7] Specifically, Cu(II) and hydroxylamine will generate hydrogen peroxide through the reduction of dissolved oxygen, which has been reported to result in greater degradation of benzoic acid compared to Cu(II) alone.[6,7] The results of these studies indicate that introduction of organic compounds that act as reducing agents can enhance the effectiveness of Cu(II) Fenton-like reactions.

In this study, we will examine the potential of Cu(II)-chitosan and Cu(II)-n-TiO_2-chitosan to participate in Fenton-like reactions to oxidize inorganic contaminants. Cu(II)-chitosan and Cu(II)-n-TiO_2-chitosan have previously been successfully utilized as adsorbents to remove As(V) and As(III).[18,21,22] As the Cu(II)-chitosan complex gains cationic behavior upon complexation of Cu(II),[18,21–25] As(V) is adsorbed through a combination of electrostatics and Lewis acid-base coordinate bonding (Figure 1A).[21,26,27] As(III), since it is neutrally charged in most environmental conditions, is adsorbed through Lewis acid-base coordinate bonding.[18,21,22,26–29]

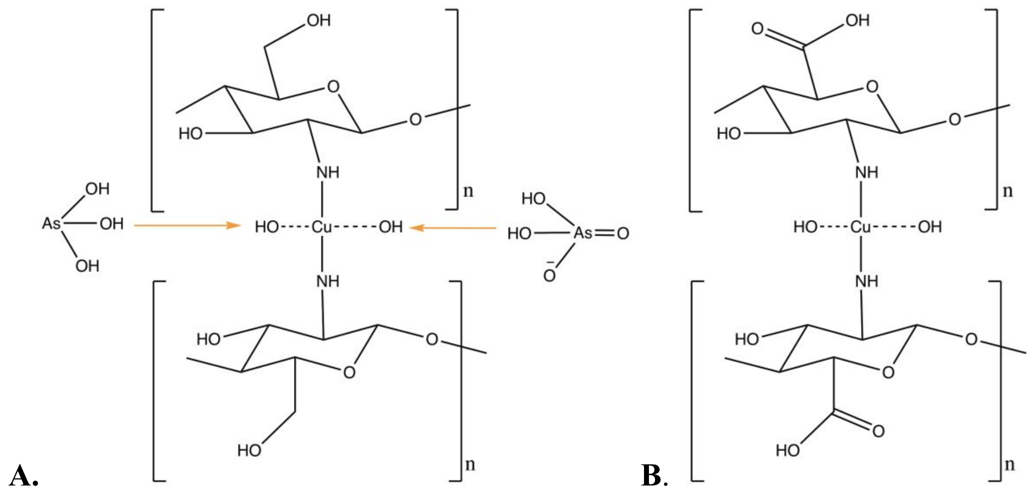

Figure 1. A. Adsorption of As(III) and As(V) by Cu(II)-chitosan. **B.** Oxidation of chitosan under UV light as proposed by Miller et al. (2011) [30].

Given the previous success utilizing Cu(II)-chitosan and Cu(II)-n-TiO_2-chitosan as adsorbents for arsenic,[18,21,22] As(III) is employed as a probe molecule to elucidate the underlying mechanism and the ability of these adsorbents to participate in Fenton-like reactions to oxidize inorganic contaminants. The effect of the Fenton-like oxidation on the arsenic removal capability of Cu(II)-chitosan and Cu(II)-n-TiO_2-chitosan is also examined.

2. Materials and Methods

Standards and Reagents

Beads of Cu(II)-chitosan and Cu(II)-n-TiO_2-chitosan were synthesized from chitosan (TCI America, 200-500 mPa-s, 0.5% in acetic acid), $Cu(NO_3)_2$-$3H_2O$ (Sigma Aldrich) and nano-TiO_2 anatase (Sigma Aldrich, < 25 nm) [21,22]. Nitric acid and sodium hydroxide used during the synthesis were prepared from a concentrated stock solution (Fisher Scientific, trace metal grade), and NaOH pellets (JT Baker, ACS reagent grade), respectively.

Arsenate stock solutions (100 ppm) were prepared using Na_2HAsO_4 -$7H_2O$ (Fisher Scientific, >99.5%), and arsenite using $NaAsO_2$ (Fluka, >99.0%). Phosphate stock solution was prepared from NaH_2PO_4 - H_2O (JT Baker, ACS reagent grade), phosphoric acid (Sigma Aldrich, trace metal grade), and DI water [21,22]. NaCl was prepared from NaCl salt (Sigma Aldrich, ACS reagent grade). HCl was prepared from concentrated stock solution (JT Baker, ACS reagent grade). Acetate buffer pH 6 (1 M) was prepared from glacial acetic acid (Fisher Scientific, ACS reagent grade) and sodium acetate anhydrous (CH_3COONa) (JT Baker, ACS reagent grade). To prepare

anoxic stock solutions, salts of As(III), As(V), NaCl, and NaOH were added to degassed water within the glovebox.

Adsorbent Synthesis

Cu(II)-chitosan and Cu(II)-n-TiO_2-chitosan were synthesized as follows by adapting the procedures of Yamani et al. (2016) and Pincus et al. (2018).[21,22] For the Cu(II)-chitosan, 0.40 g $Cu(NO_3)_2$-$3H_2O$ and 1 g chitosan were added to 0.1 M HNO_3 and stirred overnight. For Cu(II)-n-TiO_2-chitosan, after stirring overnight, n-TiO_2 was added, and the mixture stirred for another 24 hours. Two versions of Cu(II)-n-TiO_2-chitosan were synthesized, Cu(II)-n-TiO_2-chitosan A (0.40 g $Cu(NO_3)_2$-$3H_2O$, 0.30 g n-TiO_2 / g chitosan) and Cu(II)-n-TiO_2-chitosan B (0.36 g $Cu(NO_3)_2$-$3H_2O$ and 0.60 g n-TiO_2 / g chitosan). Next, a syringe pump fitted with an 18G needle was used to push droplets into 0.1 M NaOH. The solidified droplets were rinsed until filtrate was of neutral pH and then air-dried.

Arsenic Oxidation Experiments

The ability of Cu(II)-chitosan and Cu(II)-n-TiO_2-chitosan to oxidize As(III) was examined through week-long batch incubations followed by XANES analysis. For the batch experiment, 100 mg of Cu(II)-chitosan or Cu(II)-n-TiO_2-chitosan was added to 40 mL of solution in a 50-mL polypropylene falcon tube. Five systems conditions were analyzed, As(V), As(III) in dark oxic conditions, As(III) in dark anoxic conditions, As(III) + P in dark oxic conditions, and As(III) in UV light. The initial concentrations of As and P were 44 ppm As and 56 ppm P, so as to ensure full saturation of the adsorbent with arsenic resulting in a good signal to noise ratio in XANES analysis. 0.01 M NaCl was added as a background electrolyte.

Samples were incubated at 150 rpm and 25 °C for one week in VWR shaking incubators. pH was adjusted to 6 ± 0.15 daily using 0.1 M NaOH and 0.1 M HCl. For UV light incubations, an 8 W, 365 nm, UV lamp was suspended 18" above the samples. For anoxic incubations all sample preparation was done within a glovebox with a N_2 atmosphere. To prepare anoxic DI water, the freeze pump thaw method was utilized.[31] DI water was added to a sealed Schlenk tube connected to Schlenk line and frozen using liquid N_2. Once the DI water was completely frozen, the flask was opened to vacuum and then gradually thawed in room temperature water. This cycle was repeated four times before bringing the degassed DI water into the glovebox. An Extech 407510

dissolved oxygen (DO) meter (±0.4 mg/L DO accuracy) was utilized to ensure no dissolved oxygen was present in any stock or incubation solutions. For the anoxic incubations, the copper-chitosan was added to the anoxic solutions within the glovebox and all daily pH adjustments occurred within the glovebox using anoxic HCl and NaOH solutions. Following incubation, the solutions were decanted and the samples were then frozen until time of XANES analysis.

As K-edge XANES analysis

In order to assess oxidation state of arsenic present on the surface of Cu(II)-chitosan and Cu(II)-n-TiO_2-chitosan, X-ray Adsorption Near Edge Spectroscopy (XANES) was utilized. The frozen beads were sealed in Kapton tape for analysis with care taken to minimize pinholes. Anoxic samples were sealed in Kapton tape within a glovebox and then placed in a N_2 atmosphere glovebag during analysis.

XANES spectra were collected at the As K-edge (11867 eV) and Cu K-edge (8979 eV) at the Inner Shell Spectroscopy beamline (8-ID) at the National Synchrotron Light Source II (NSLS II) at Brookhaven National Laboratory and the As K-edge at beamline 9-BM at the Advanced Photon Source (APS) at Argonne National Laboratory. As K-edge spectra were calibrated to the Au L-edge (11919 eV) using an Au reference foil.[32] Cu K-edge spectra were calibrated using a Cu foil. Multiple scans were collected and averaged to improve the signal to noise ratio. At NSLS II, the electron storage ring operated at 3 GeV with a 400 mA beam current. Spectra were acquired in fluorescence mode at room temperature using a cryogenically cooled Si (111) Double Crystal monochromator and a Passivated Implanted Planar Silicon (PIPS) detector. A germanium Z-1 filter was used to suppress the elastic scattering on the detector. At APS, the electron storage ring operated at 7 GeV with a 100 mA beam current. Samples were kept at 20 K using a liquid helium flow cryostat and spectra acquired in florescence mode using a 4-element Vortex Silicon Drift Detector (SDD).

Data reduction and analysis were performed using the Athena program.[33] Linear combination fitting (LCF) performed using the Athena program was used to determine relative percentages of arsenate and arsenite adsorbed to each sample.[33,34] The standards used for As(III) and As(V) were 100 mMol solutions of sodium arsenite and sodium arsenate dibasic heptahydrate, respectively. Uncertainties of fit reported were calculated by Athena as R-Factor = $\Sigma(\text{data} - \text{fit})^2$ / $\Sigma(\text{data}^2)$, where an R-Factor < 0.05 is considered a reasonable fit.[33,35]

178

179 *Arsenic Adsorption Experiments*

180 Week-long batch incubations were utilized in order to examine the arsenic removal
181 capability.[12,18,21,22,30,36,37] The adsorbents were added to 40 mL of solution in a 50-mL
182 polypropylene Falcon tube. The following systems conditions were analyzed: As(V) dark,
183 As(V)+P dark, As(III) dark, As(III)+P dark, As (III) UV, As (III)+P UV, and As(III) dark
184 anoxic. In each systems condition, the initial concentration of arsenic was varied. Phosphate was
185 chosen as a competitive oxyanion due to its ability to strongly compete with arsenic for
186 adsorption sites.[38] When phosphate was present, the initial concentration was 16 ppm. A 25 mM
187 acetate buffer pH 6 was added to maintain constant pH.[18,21,22] All anoxic experiments were done
188 in an N_2 atmosphere using the methods described in Section 2.3. The incubation methods also
189 follow the procedure outlined in Section 2.3 except that daily pH adjustments were not done due
190 to the use of the acetate buffer pH 6.

191 Prior to analysis, samples were filtered using a 0.22-μm PVDF filter and diluted with 1%
192 nitric acid. A Perkin Elmer DRC-e inductively coupled plasma-mass spectrometry (ICP-MS) was
193 used to analyze the samples. A Scott Crossflow nebulizer with mixing tee, Argon plasma, and
194 germanium and scandium internal standards were utilized during the analysis.[21,22] Triplicate
195 analyses were performed with a repeating standard and blank every ten samples to track
196 instrument stability.

197

198 3. Results and Discussion

199 3.1 Assessment of As oxidation state via As K-edge XANES

200 As K-edge XANES were utilized to analyze speciation of arsenic adsorbed to the surface of
201 Cu (II)-chitosan. E_0, measured as the white line, was found to be 11871.7 eV for As(III) and
202 11875.1 eV for As(V) (Figure 2). By fitting XANES spectra to liquid standards of 100 mMol
203 As(III) and As(V) using LCF analysis in Athena, the relative speciation of adsorbed arsenic can
204 be quantified.[33,34] R-factors below 0.05 indicate goodness of fit by LCF (Table 1).[33,35]

205 As K-edge XANES indicate that As(V) does not undergo any redox reactions upon binding
206 to Cu(II)-chitosan and is adsorbed as As(V) (Figure 2, Table 1). In contrast, As(III) is fully
207 oxidized to As(V) (100% ± 0.0) upon binding to Cu(II)-chitosan in the dark in oxic conditions.

This result confirms that Cu(II)-chitosan is capable of oxidizing As(III) to As(V) without the addition of a photo- or chemical-oxidant.

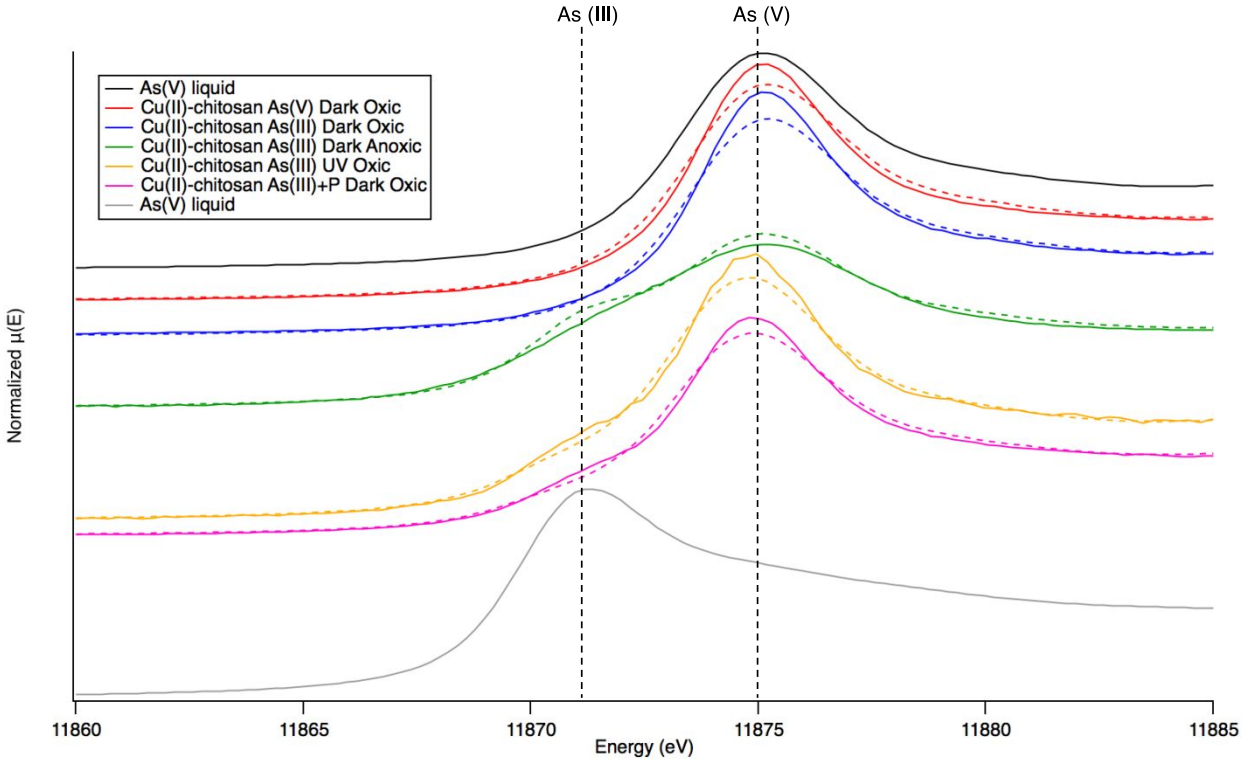

Figure 2. Stacked and normalized As K-edge XANES spectra for Cu(II)-chitosan (0.4 g Cu / g chitosan) incubated in various systems conditions and 100 mMol As(V) and As(III) liquid standards. Data is shown with solid lines, fits generated by LCF analysis in Athena are shown as dashed lines.

Table 1. Results of Linear Combination Fitting Showing Combinations of Standards Yielding the Best Fits to Cu(II)-Chitosan Arsenic K-Edge XANES

System Condition	% As(V)	% As(III)	R-Factor[a]
As V Dark Oxic	100 ± 0.0	0.00 ± 0.0	0.007
As IIII Dark Oxic	100 ± 0.0	0.00 ± 0.0	0.009
As III Dark Anoxic	60.2 ± 0.1	39.8 ± 0.1	0.005
As III UV Oxic	86.9 ± 0.1	13.1 ± 0.1	0.008
As III + P Dark Oxic	90.0 ± 0.1	10.0 ± 0.1	0.005

[a]Uncertainties of fit reported were calculated by Athena as R-Factor = $\Sigma(\text{data} - \text{fit})^2 / \Sigma(\text{data}^2)$.

As K-edge XANES analysis of Cu(II)-n-TiO_2-chitosan A (0.4 g $Cu(NO_3)_2$-$3H_2O$, 0.30 g n-TiO_2 / g chitosan) and Cu(II)-n-TiO_2-chitosan B (0.36 g $Cu(NO_3)_2$-$3H_2O$ and 0.60 g n-TiO_2 / g chitosan) was also performed (Figure 3). As expected, no redox transformations were observed post-adsorption of As(V) by Cu(II)-n-TiO_2-chitosan A or B (Figure 3, Table 2). Following incubation in UV light, As(III) was fully photo-oxidized to As(V) by Cu(II)-n-TiO_2-chitosan A and B prior to adsorption, and thus, is bound fully as As(V). This is expected since n-TiO_2 is a

known photo-oxidant of As(III) in UV light.[12,18,21,30,36,39,40] Interestingly, following incubation in darkness, As(III) is present on the surface of Cu(II)-n-TiO_2-chitosan A and B as a mixture of As(III) and As(V) (Figure 3). For Cu(II)-n-TiO_2-chitosan A, As(III) was present as 50.7 ± 0.1% As(V) (Table 2). In contrast, Cu(II)-n-TiO_2-chitosan B had only 17.3 ± 0.1% As(V) present on the surface. The amount of As(V) vs As(III) on the surface of both beads correlates with the relative loading of Cu(II) rather than n-TiO_2.

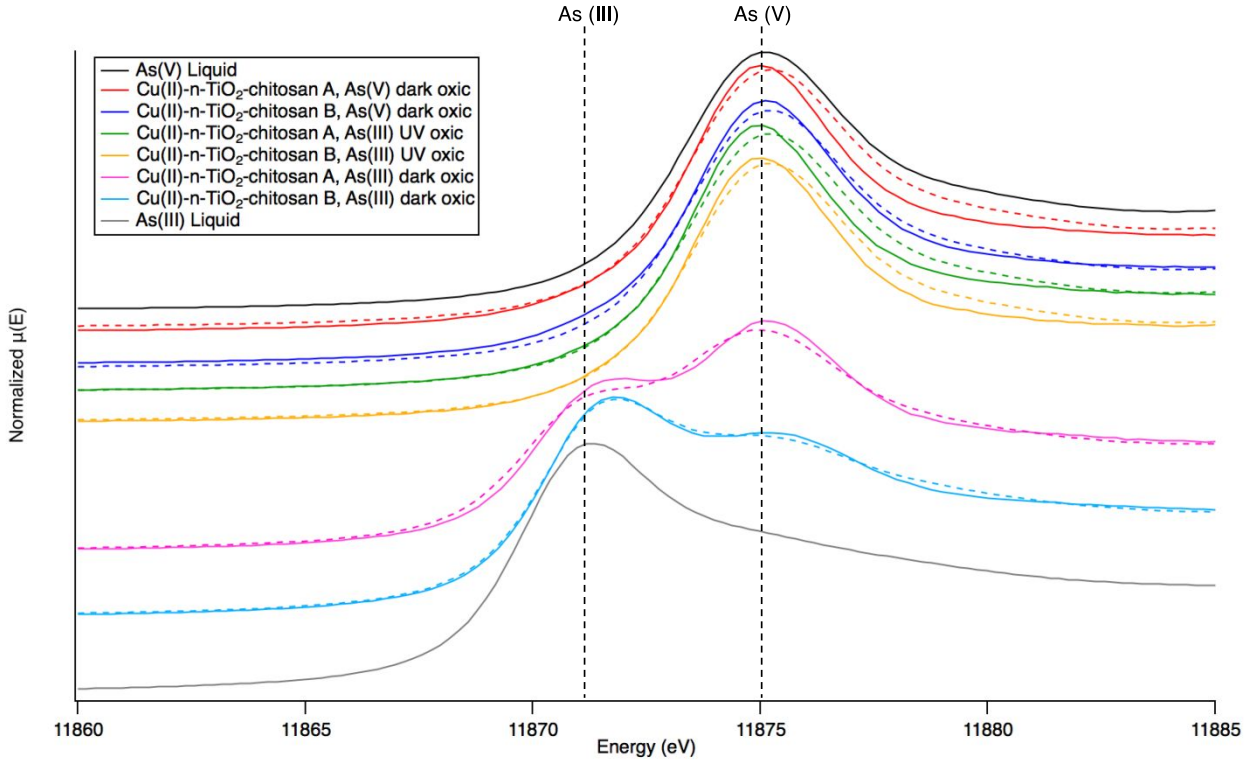

Figure 3. Stacked and normalized As K-edge XANES spectra for Cu(II)-n-TiO_2-chitosan A (0.40 g Cu, 0.30 g nTiO_2 / g chitosan) and Cu(II)-n-TiO_2-chitosan B (0.36 g Cu, 0.60 g nTiO_2 / g chitosan) incubated in various systems conditions and 100 mMol As(V) and As(III) liquid standards. Data is shown with solid lines, fits generated by LCF analysis in Athena are shown as dashed lines.

Table 2. Results of Linear Combination Fitting Showing Combinations of Standards Yielding the Best Fits to Cu(II)-n-TiO_2-Chitosan Arsenic K-Edge XANES

Sample	System Condition	% As(V)	% As(III)	R-Factor[a]
Cu(II)-n-TiO_2 A	As V Dark Oxic	100 ± 0.0	0.00 ± 0.0	0.008
	As III UV Oxic	100 ± 0.0	0.00 ± 0.0	0.009
	As IIII Dark Oxic	50.7 ± 0.1	49.3 ± 0.1	0.004
Cu(II)-n-TiO_2 B	As V Dark Oxic	100 ± 0.0	0.00 ± 0.0	0.005
	As III UV Oxic	100 ± 0.0	0.00 ± 0.0	0.008
	As IIII Dark Oxic	17.3 ± 0.1	82.7 ± 0.1	0.001

[a]Uncertainties of fit reported were calculated by Athena as R-Factor = $\Sigma(data - fit)^2 / \Sigma(data^2)$.

242
243
244 3.2 Oxidation of As(III) to As(V) via Fenton-like reaction mechanism
245 In order to assess the role of dissolved oxygen in the reaction mechanism, an incubation was
246 conducted in a N_2 atmosphere with stock solutions degassed using the freeze pump thaw
247 method.[31] Upon removal of dissolved oxygen, As(III) is adsorbed to Cu(II)-chitosan as a mixture
248 of As(V) (60.2 ± 0.1%) and As(III) (39.8± 0.1%), as compared to in oxic conditions where
249 As(III) is bound to Cu(II)-chitosan 100% ± 0.0% as As(V) (Figure 2, Table 1). The inhibitory
250 effect of removal of dissolved oxygen suggests that oxidation of As(III) to As(V) occurs through
251 a Cu(II)-chitosan Fenton-like reaction.[8,41]
252 It is hypothesized that in this Fenton-like reaction, chitosan acts as a reducing agent, similar
253 to hydroxyl amine, accelerating the rate of Cu(II) reduction and production of hydrogen peroxide
254 from dissolved oxygen.[7,42] The H_2O_2, then forms reactive complexes with Cu(II)-chitosan to
255 produce hydroxyl radicals and Cu(III).[6,41] These reactive oxidants in turn oxidize As(III) to
256 As(V). Overall, the proposed mechanism in the system is that Cu(II)-chitosan/O_2 act as a two-
257 electron oxidant oxidizing As(III) to As(V) and reducing dissolved O_2 to H_2O (Figure 4).[41]
258 While this specific reaction mechanism has not been previously analyzed, these results agree
259 with earlier studies of related Fenton and Fenton-like reactions where it has been shown that
260 Cu(II) Fenton-type reactions with H_2O_2 or hydroxylamine serving as the reducing agent are
261 capable of oxidizing various organic compounds such as acetaminophen,[8] benzoate,[6,7] phenol,[6]
262 and methanol.[6] Oxidation of As(III) to As(V) via Fe(II)/H_2O_2 systems where hydrogen peroxide
263 is the reducing agent have been previously analyzed and found to be successful.[6,19] However, a
264 Cu(II)/H_2O_2 systems comprised of 0.1 mM Cu(II) ions and 0.2 mM H_2O_2 was found to be
265 unsuccessful for oxidation of As(III) in a study by Lee et al. (2013). This suggests the
266 importance of chitosan as a reducing agent in the system to enhance the rate of Cu(II) reduction
267 within the Cu(II)-chitosan oxidation mechanism.[7,42]
268

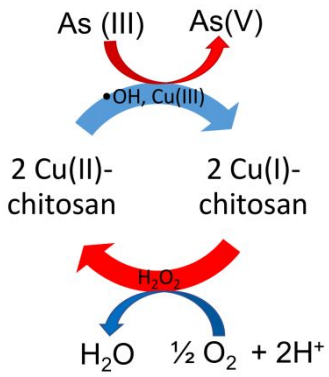

Figure 4. Proposed mechanism for As(III) oxidation by Cu(II)-chitosan through a Fenton-like reaction. Blue arrows indicate reduction reactions and red arrows indicate oxidation reactions.

3.3 Inhibition of As(III) oxidation by UV light and phosphate

Incubation in UV light resulted in slight inhibition of the As(III) oxidation with As(III) bound on the surface as 86.9 ± 0.1 % As(V) and 13.1 ± 0.1% As(III) (Figure 2, Table 1). UV light is known to affect the structure of chitosan, transforming hydroxyl groups into carboxyl groups (Figure 1B).[30,43] Thus, structural changes to the chitosan backbone have a negative effect on the ability of Cu(II)-chitosan to oxidize As(III) to As(V), suggesting the involvement of chitosan in this oxidation reaction.

Addition of phosphate had a slight inhibitory effect on the oxidation of As(III), decreasing %As(III) oxidized to As(V) from 100% ± 0.0% to 90.0 ± 0.1% (Figure 2, Table 2). This inhibitory effect is potentially due to poisoning of Cu(II) as a catalyst by phosphate. While not yet demonstrated for Cu(II)-chitosan or specifically for Fenton-like reactions, phosphate is known to inhibit Cu(II)-catalysis.[44,45]

3.4 Analysis of copper oxidation state via Cu K-edge XANES

To confirm the role of Cu(II) as a catalyst, Cu K-edge X-ray adsorption near edge spectroscopy (XANES) were utilized to analyze the oxidation state of Cu within Cu(II)-chitosan under various systems conditions. The oxidation state of copper was unaffected by changes in system conditions, remaining bound as Cu(II) for incubation in As(V), As(III) oxic conditions, and As(III) anoxic conditions (Figure 5). As these XANES analyses were conducted once the As(III)-Cu(II)-chitosan system reached equilibrium, it would be expected that Cu(II) would be present as Cu(II) given its role as a catalyst that would be regenerated at the end of the oxidation reaction, rather than a reactant.

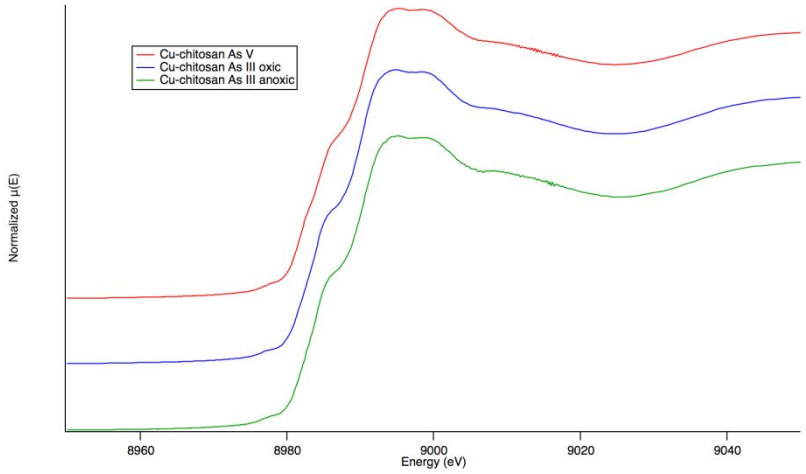

Figure 5. Stacked and normalized Cu K-edge XANES spectra for Cu(II)-chitosan (0.4 g Cu / g chitosan) incubated in various systems conditions.

3.4 Analysis of arsenic removal potential of Cu(II)-chitosan and Cu(II)-n-TiO_2-chitosan

In order to assess the effect of the observed redox reactions on arsenic removal potential by these adsorbents, adsorption isotherms were generated for Cu(II)-chitosan (Figure 6), and the two versions (A and B) of Cu(II)-n-TiO_2 chitosan in all systems conditions (As(V), As(V) + P, As(III) dark, As(III) + P dark, As(III) UV, As(III) + P UV, and As(III) anoxic) (Figure S2 and S3). Langmuir (solid fits) and Freundlich (dashed fits) adsorption theory was used to model the data in order to determine which model more closely describes adsorption behavior. The equations of these two models can be found within the supplemental information.

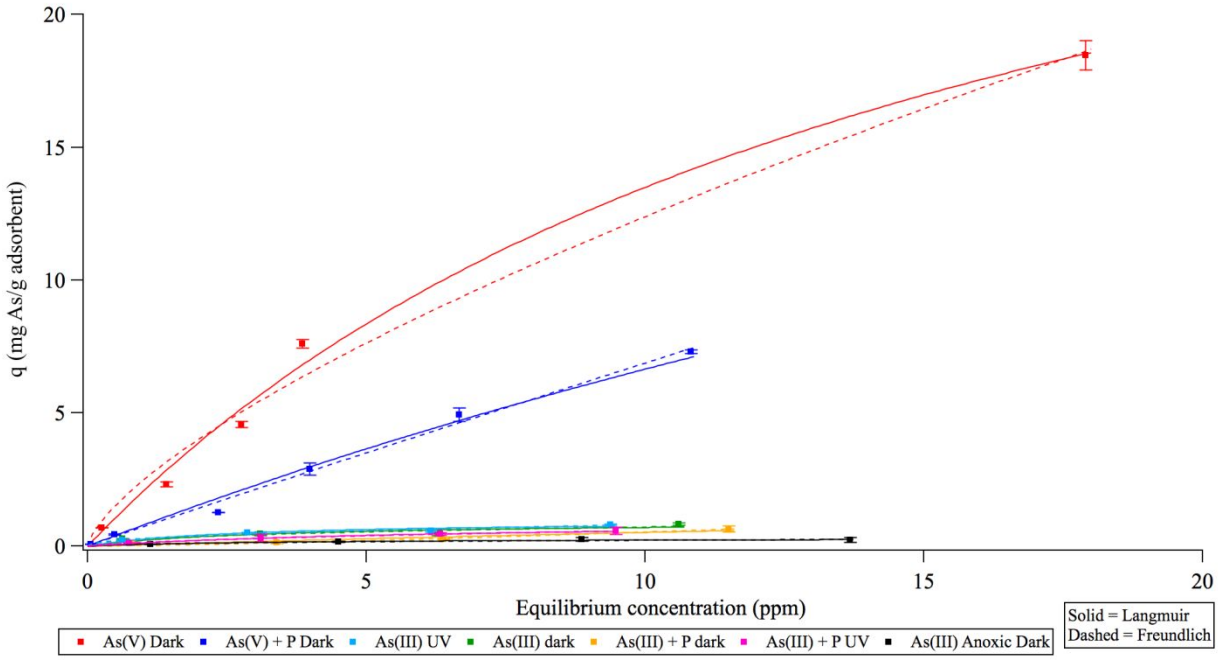

	As(V) Dark	As(V) + P Dark	As(III) UV	As(III) + P UV	As(III) Dark	As(III) + P Dark	As(III) Anoxic Dark
Langmuir							
q Max (mg/g)	35.0	37.2	0.959	0.964	0.930	0.964	0.310
b (L/mg)	0.063	0.022	0.380	0.144	0.304	0.144	0.266
Chi-square	1.25	0.390	0.013	0.001	0.063	0.001	0.001
Freundlich							
K_f	2.48	0.730	0.290	0.145	0.263	0.024	0.082
1/n	0.698	0.975	0.451	0.608	0.438	1.34	0.427
Chi-square	2.52	0.287	0.007	0.001	0.038	0.012	0.003

Figure 6. Adsorption isotherms and fitting parameters for arsenic removal of Cu-chitosan chitosan (0.4 g $Cu(NO_3)_2$-$3H_2O$ per 1 g chitosan). Initial As concentrations were 1, 4, 8, and 12 ppm and 0.25 mM acetate buffer pH 6, for all systems except As(V) where 1, 2, 4, 8, and 40 ppm were the initial As concentrations. Phosphate concentration was 16 ppm when present. 8 W, 365 nm UV light was used where indicated. Anoxic incubation was done in a N atmosphere. Langmuir fits indicated with solid lines and Freundlich fits with dashed lines.

Overall results agree with previous findings[21,22] that Cu(II)-chitosan is capable of selective adsorption of As(V) over phosphate. The highest As removal performance by Cu(II)-chitosan was of As(V), followed by As(V) + P (Figure 6). The remaining systems conditions had relatively low arsenic removal performance. There were slight differences in arsenic removal capability with slightly higher removal of As(III) UV followed by (listed in order of decreasing As removal performance): As(III) dark, As(III) + P dark, As(III) + P UV, and As(III) anoxic dark. All systems, with the exception of As(V), As(III) + P UV, and As(III) + P dark, were better described by the Freundlich model, as indicated by lower chi-square values. As(V) and As(III) + P dark removal performance was better described by the Langmuir model and a similar quality

fit was obtained using both models for As(III) + P UV. Adsorption isotherms for Cu(II)-n-TiO_2-chitosan A and B are found within the SI (Figure S2 and S3).

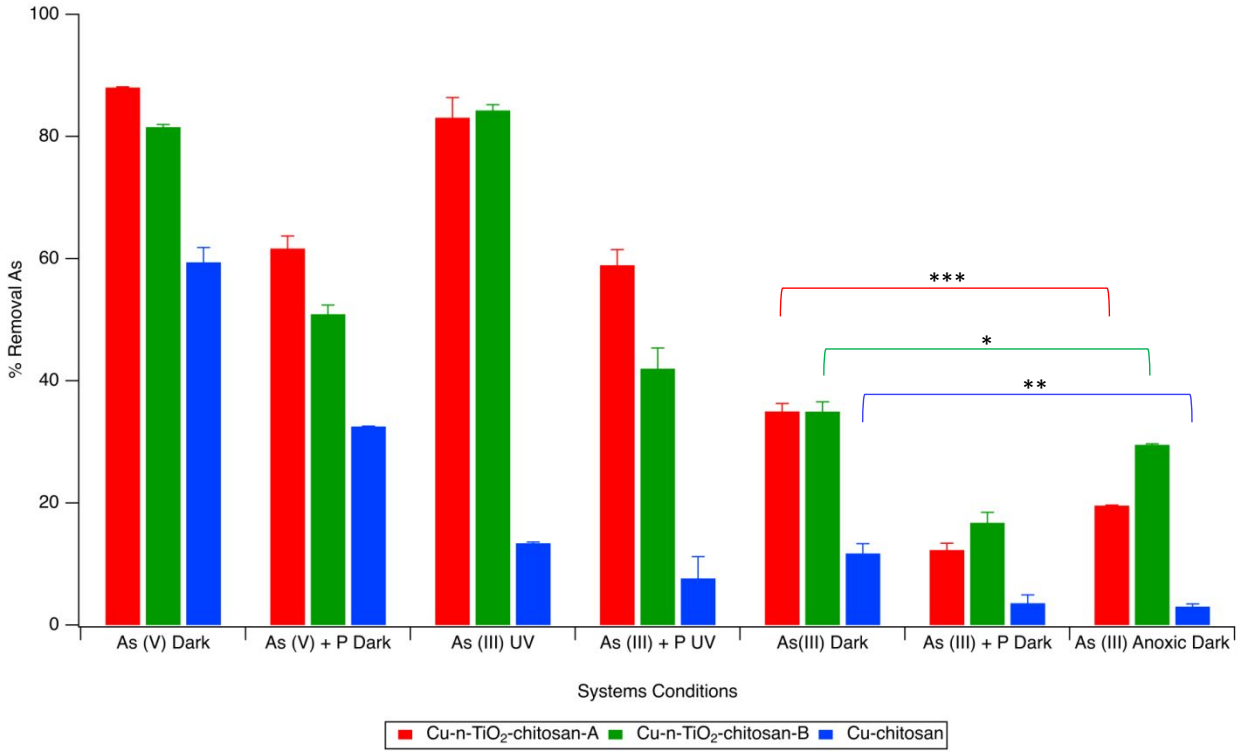

Figure 7. Comparison of Cu-n-TiO_2-chitosan-A (0.4 g $Cu(NO_3)_2$-$3H_2O$, 0.3 g n-TiO_2 loading / 1 g chitosan), Cu-n-TiO_2-chitosan-B (0.36 g $Cu(NO_3)_2$-$3H_2O$, 0.6 g n-TiO_2 / 1 g chitosan), and Cu-chitosan (0.4 g $Cu(NO_3)_2$-$3H_2O$ per 1 g chitosan) performance. Initial concentrations were 4 ppm As and 25 mM acetate buffer pH 6, and 16 ppm P when present. Where indicated an 8W 365 nm UV light was used. Anoxic incubation was done in a N atmosphere. T-test at 95% confidence level ($p < 0.05$) showed that these changes in As(III) removal are statistically significant for Cu(II)-chitosan **(p value = 0.035) and Cu(II)-n-TiO_2-chitosan-A ***(p value = 0.007), but not Cu(II)-TiO_2-chitosan B *(p value = 0.07) which contained more n-TiO_2 than Cu(II), so was less affected by the change in environmental conditions.

Comparing all three adsorbents, the adsorbent with the greatest arsenic removal capability in all systems conditions examined was Cu(II)-n-TiO_2-chitosan A followed by Cu(II)-n-TiO_2-chitosan B, and finally Cu(II)-chitosan (Figure 7). Cu(II)-n-TiO_2-chitosan A outperformed Cu(II)-n-TiO_2 B due to it having more optimal ratios of both active components (Cu and n-TiO_2), enough Cu(II) to selectively remove As and enough n-TiO_2 to effectively photo-oxidize As(III) to the more easily adsorbed As(V).[18,21] Cu(II)-chitosan was not as effective at arsenic removal due to its inability to photo-oxidize As(III) to As(V) in UV light.

Critically, it was found that the observed Fenton-like reaction significantly impacts the adsorption capacity of Cu(II)-chitosan and Cu(II)-n-TiO_2-chitosan towards As(III). Comparing

As(III) removal in oxic and anoxic conditions, Cu(II)-n-TiO_2-chitosan A saw a 75% increase (35% up from 20%,) in As(III) removal in oxic vs anoxic conditions and Cu(II)-n-TiO_2-chitosan B a 16% increase (35% up from 30%). Similarly, Cu(II)-chitosan removed 11.8% of As(III) in oxic conditions, but only 3.1% in anoxic conditions, suggesting a 280% increase in As(III) removal capability.

Likely, the decreased effect of anoxic conditions on As(III) removal by Cu(II)-n-TiO_2-chitosan B is due to its lower loading of Cu(II) and higher loading of n-TiO_2 compared to both Cu(II)-n-TiO_2-chitosan A and Cu(II)-chitosan. As suggested by the XANES analyses (Figure 3), if oxidation of As(III) to As(V) via the proposed Fenton-like mechanism occurs solely at Cu(II) binding sites, then we would expect that the higher loading of n-TiO_2-chitosan in adsorbent B would lead to less Fenton-like oxidation of As(III). Thus, the change from oxic to anoxic conditions has less of an effect on As(III) removal for Cu(II)-n-TiO_2-chitosan B than Cu(II)-n-TiO_2-chitosan A and Cu(II)-chitosan. Cu(II)-n-TiO_2-chitosan A is less affected than Cu(II)-chitosan as it does have some n-TiO_2 binding sites for As(III) which will not be affected by the change from oxic to anoxic conditions.

3.5 Conclusion

Through this work we have observed that Cu(II)-chitosan is capable of effectively oxidizing As(III) to As(V) through a Fenton-like reaction. Both Cu(II) and chitosan contribute to this reaction mechanism, Cu(II) as a catalyst, and chitosan as a reducing agent. This oxidation reaction significantly enhances the As(III) removal performance of Cu(II)-chitosan and Cu(II)-n-TiO_2-chitosan. The ability of Cu(II)-chitosan and Cu(II)-n-TiO_2-chitosan to oxidize As(III) to As(V) simultaneous with arsenic removal enables the elimination of a traditional pre-treatment oxidation step, and thus, may increase the cost efficiency of these adsorbents compared to traditional non-multifunctional materials. The use of chitosan, a natural waste product of the shellfish industry, also has the potential to enhance cost-effectiveness of these adsorbents.

Increased understanding of As(III) oxidation via Fenton-like reactions could help to elucidate arsenic interactions with metal-organic complexes in aqueous and terrestrial environments, as well as within the human body. As arsenic is a probe molecule to explore the mechanism of Cu(II)-chitosan Fenton-like reactions, this system has widespread potential uses in participating in redox reactions of other inorganic contaminants of interest such as elemental

mercury and hexavalent chromium. Fenton-like reactions hold great promise in their ability to oxidize or reduce inorganic contaminants (e.g. chromium) into their less toxic and/or more easily removed oxidation states.

Increased knowledge about the ability of Fenton and Fenton-like reactions to oxidize inorganic contaminants will enable their use within more realistic, mixed organic/inorganic contaminant systems. Fenton and Fenton-like reactions have been widely utilized to oxidize organic compounds into less toxic or more easily biodegradable molecules, however oxidation of inorganics has been much less frequently studied. Incorporation of a simultaneous ability to oxidize inorganics and organics, without the need for an external oxidant such as H_2O_2 or UV light, can increase the economic feasibility of these oxidation techniques as well as the variety of systems in which these techniques will be effective.

Acknowledgements

This work was supported by the NSF Nanosystems Engineering Research Center for Nanotechnology-Enabled Water Treatment (ERC-1449500). We would like to thank Dr. Jonas Karosas and the Yale Analytical and Stable Isotope Center for his help and use of the ICP-MS. We thank Dr. George E. Sterbinsky at APS 9-BM for use of the beamlines and assistance with our project. We also thank Dr. Aaron Bloomfield, Dr. Amanda Lounsbury, Eva Albalghiti, Mary Kate Mitchell Lane, Holly Rudel, and Dr. Tamara Winter for their help with this project. This research used the Inner Shell Spectroscopy beamline (8-ID) of the National Synchrotron Light Source II, a U.S. Department of Energy (DOE) Office of Science User Facility operated for the DOE Office of Science by Brookhaven National Laboratory under Contract No. DE-SC0012704. This research used resources of the Advanced Photon Source, a U.S. Department of Energy (DOE) Office of Science User Facility operated for the DOE Office of Science by Argonne National Laboratory under Contract No. DE-AC02- 06CH11357.

References

1 A. D. Bokare and W. Choi, Review of iron-free Fenton-like systems for activating H2O2 in advanced oxidation processes, *J. Hazard. Mater.*, 2014, **275**, 121–135.

2 J. J. Pignatello, E. Oliveros and A. MacKay, Advanced Oxidation Processes for Organic Contaminant Destruction Based on the Fenton Reaction and Related Chemistry, *Crit. Rev. Environ. Sci. Technol. Boca Raton*, 2006, **36**, 1–84.

3 I. A. Katsoyiannis, T. Ruettimann and S. J. Hug, pH Dependence of Fenton Reagent Generation and As(III) Oxidation and Removal by Corrosion of Zero Valent Iron in Aerated Water, *Environ. Sci. Technol.*, 2008, **42**, 7424–7430.

4 L. Wang and D. E. Giammar, Effects of pH, dissolved oxygen, and aqueous ferrous iron on the adsorption of arsenic to lepidocrocite, *J. Colloid Interface Sci.*, 2015, **448**, 331–338.

5 A. Mirzaei, Z. Chen, F. Haghighat and L. Yerushalmi, Removal of pharmaceuticals from water by homo/heterogonous Fenton-type processes – A review, *Chemosphere*, 2017, **174**, 665–688.

6 H. Lee, H.-J. Lee, D. L. Sedlak and C. Lee, pH-Dependent reactivity of oxidants formed by iron and copper-catalyzed decomposition of hydrogen peroxide, *Chemosphere*, 2013, **92**, 652–658.

7 H. Lee, H.-J. Lee, J. Seo, H.-E. Kim, Y. K. Shin, J.-H. Kim and C. Lee, Activation of Oxygen and Hydrogen Peroxide by Copper(II) Coupled with Hydroxylamine for Oxidation of Organic Contaminants, *Environ. Sci. Technol.*, 2016, **50**, 8231–8238.

8 Y. Zhang, J. Fan, B. Yang, W. Huang and L. Ma, Copper–catalyzed activation of molecular oxygen for oxidative destruction of acetaminophen: The mechanism and superoxide-mediated cycling of copper species, *Chemosphere*, 2017, **166**, 89–95.

9 S. Lata and S. R. Samadder, Removal of arsenic from water using nano adsorbents and challenges: A review, *J. Environ. Manage.*, 2016, **166**, 387–406.

10 D. Mohan and C. U. Pittman Jr., Arsenic removal from water/wastewater using adsorbents—A critical review, *J. Hazard. Mater.*, 2007, **142**, 1–53.

11 P. L. Smedley and D. G. Kinniburgh, A review of the source, behaviour and distribution of arsenic in natural waters, *Appl. Geochem.*, 2002, **17**, 517–568.

12 J. S. Yamani, S. M. Miller, M. L. Spaulding and J. B. Zimmerman, Enhanced arsenic removal using mixed metal oxide impregnated chitosan beads, *Water Res.*, 2012, **46**, 4427–4434.

13 S. Goldberg and C. T. Johnston, Mechanisms of Arsenic Adsorption on Amorphous Oxides Evaluated Using Macroscopic Measurements, Vibrational Spectroscopy, and Surface Complexation Modeling, *J. Colloid Interface Sci.*, 2001, **234**, 204–216.

14 M. Bissen and F. H. Frimmel, Arsenic — a Review. Part II: Oxidation of Arsenic and its Removal in Water Treatment, *Acta Hydrochim. Hydrobiol.*, 2003, **31**, 97–107.

15 M. A. Ferguson, M. R. Hoffmann and J. G. Hering, TiO2-Photocatalyzed As(III) Oxidation in Aqueous Suspensions: Reaction Kinetics and Effects of Adsorption, *Environ. Sci. Technol.*, 2005, **39**, 1880–1886.

16 X. Guan, J. Du, X. Meng, Y. Sun, B. Sun and Q. Hu, Application of titanium dioxide in arsenic removal from water: A review, *J. Hazard. Mater.*, 2012, **215–216**, 1–16.

17 H. Lee and W. Choi, Photocatalytic Oxidation of Arsenite in TiO2 Suspension: Kinetics and Mechanisms, *Environ. Sci. Technol.*, 2002, **36**, 3872–3878.

18 L. N. Pincus, A. W. Lounsbury and J. B. Zimmerman, Toward Realizing Multifunctionality: Photoactive and Selective Adsorbents for the Removal of Inorganics in Water Treatment, *Acc. Chem. Res.*, , DOI:10.1021/acs.accounts.8b00668.

19 S. J. Hug and O. Leupin, Iron-Catalyzed Oxidation of Arsenic(III) by Oxygen and by Hydrogen Peroxide: pH-Dependent Formation of Oxidants in the Fenton Reaction, *Environ. Sci. Technol.*, 2003, **37**, 2734–2742.

20 L.-C. Hsu, K.-Y. Chen, Y.-T. Chan, Y. Deng, C.-E. Hwang, Y.-T. Liu, S.-L. Wang, W.-H. Kuan and Y.-M. Tzou, MS title: Catalytic oxidation and removal of arsenite in the presence of Fe ions and zero-valent Al metals, *J. Hazard. Mater.*, 2016, **317**, 237–245.

21 L. N. Pincus, F. Melnikov, J. S. Yamani and J. B. Zimmerman, Multifunctional photoactive and selective adsorbent for arsenite and arsenate: Evaluation of nano titanium dioxide-enabled chitosan cross-linked with copper, *J. Hazard. Mater.*, 2018, **358**, 145–154.

22 J. S. Yamani, A. W. Lounsbury and J. B. Zimmerman, Towards a selective adsorbent for arsenate and selenite in the presence of phosphate: Assessment of adsorption efficiency, mechanism, and binary separation factors of the chitosan-copper complex, *Water Res.*, 2016, **88**, 889–896.

23 E. Guibal, N. Von Offenberg Sweeney, M. C. Zikan, T. Vincent and J. M. Tobin, Competitive sorption of platinum and palladium on chitosan derivatives, *Int. J. Biol. Macromol.*, 2001, **28**, 401–408.

24 R. Lü, Z. Cao and G. Shen, Comparative study on interaction between copper (II) and chitin/chitosan by density functional calculation, *J. Mol. Struct. THEOCHEM*, 2008, **860**, 80–85.

25 S. Qian, G. Huang, J. Jiang, F. He and Y. Wang, Studies of adsorption behavior of crosslinked chitosan for Cr(VI), Se(VI), *J. Appl. Polym. Sci.*, 2000, **77**, 3216–3219.

26 B. An, T. R. Steinwinder and D. Zhao, Selective removal of arsenate from drinking water using a polymeric ligand exchanger, *Water Res.*, 2005, **39**, 4993–5004.

27 B. An, Z. Fu, Z. Xiong, D. Zhao and A. K. SenGupta, Synthesis and characterization of a new class of polymeric ligand exchangers for selective removal of arsenate from drinking water, *React. Funct. Polym.*, 2010, **70**, 497–507.

28 Ramana Anuradha and Sengupta Arup K., Removing Selenium(IV) and Arsenic(V) Oxyanions with Tailored Chelating Polymers, *J. Environ. Eng.*, 1992, **118**, 755–775.

29 W. Tao, A. Li, C. Long, Z. Fan and W. Wang, Preparation, characterization and application of a copper (II)-bound polymeric ligand exchanger for selective removal of arsenate from water, *J. Hazard. Mater.*, 2011, **193**, 149–155.

30 S. M. Miller, M. L. Spaulding and J. B. Zimmerman, Optimization of capacity and kinetics for a novel bio-based arsenic sorbent, TiO2-impregnated chitosan bead, *Water Res.*, 2011, **45**, 5745–5754.

31 J. Eastoe and C. Ellis, De-gassed water and surfactant-free emulsions: History, controversy, and possible applications, *Adv. Colloid Interface Sci.*, 2007, **134–135**, 89–95.

32 K. Müller, V. S. T. Ciminelli, M. S. S. Dantas and S. Willscher, A comparative study of As(III) and As(V) in aqueous solutions and adsorbed on iron oxy-hydroxides by Raman spectroscopy, *Water Res.*, 2010, **44**, 5660–5672.

33 B. Ravel and M. Newville, ATHENA, ARTEMIS, HEPHAESTUS: data analysis for X-ray absorption spectroscopy using IFEFFIT, *J. Synchrotron Radiat.*, 2005, **12**, 537–541.

34 Y. Arai, E. J. Elzinga and D. L. Sparks, X-ray Absorption Spectroscopic Investigation of Arsenite and Arsenate Adsorption at the Aluminum Oxide–Water Interface, *J. Colloid Interface Sci.*, 2001, **235**, 80–88.

35 D. V. Babos, J. P. Castro, D. F. Andrade, V. C. Costa and E. R. Pereira-Filho, Determination and speciation of phosphorus in fertilizers and mineral supplements for cattle by X-ray absorption near-edge structure spectroscopy: a simple nondestructive method, *Anal. Methods*, 2019, **11**, 1508–1515.

36 S. M. Miller and J. B. Zimmerman, Novel, bio-based, photoactive arsenic sorbent: TiO2-impregnated chitosan bead, *Water Res.*, 2010, **44**, 5722–5729.

37 J. S. Yamani, A. W. Lounsbury and J. B. Zimmerman, Adsorption of selenite and selenate by nanocrystalline aluminum oxide, neat and impregnated in chitosan beads, *Water Res.*, 2014, **50**, 373–381.

38 L. Pincus, H. Rudel, P. Petrovic, S. Gupta, P. Westerhoff, C. Muhich and J. B. Zimmerman, Exploring the Mechanisms of Selectivity for Environmentally Significant Oxo-anion Removal During Water Treatment: a Review of Common Competing Oxo-anions and Tools for Quantifying Selective Adsorption, *Environ. Sci. Technol.*, 2020, acs.est.0c01666.

39 M. Bissen, M.-M. Vieillard-Baron, A. J. Schindelin and F. H. Frimmel, TiO2-catalyzed photooxidation of arsenite to arsenate in aqueous samples, *Chemosphere*, 2001, **44**, 751–757.

40 S. Bang, M. Patel, L. Lippincott and X. Meng, Removal of arsenic from groundwater by granular titanium dioxide adsorbent, *Chemosphere*, 2005, **60**, 389–397.

41 S. D. McCann and S. S. Stahl, Copper-Catalyzed Aerobic Oxidations of Organic Molecules, https://pubs.acs.org/doi/abs/10.1021/acs.accounts.5b00060, (accessed 6 April 2018).

42 J. F. Perez-Benito, Reaction pathways in the decomposition of hydrogen peroxide catalyzed by copper(II), *J. Inorg. Biochem.*, 2004, **98**, 430–438.

43 G. A.-W. Ahmed, K. S. Khairou and R. M. Hassan, Kinetics and mechanism of oxidation of Chitosan Polysaccharide by Permanganate Ion in Aqueous Perchlorate Solutions, *J. Chem. Res.*, 2003, **2003**, 182–183.

44 H. Tounsi, S. Djemal, C. Petitto and G. Delahay, Copper loaded hydroxyapatite catalyst for selective catalytic reduction of nitric oxide with ammonia, *Appl. Catal. B Environ.*, 2011, **107**, 158–163.

45 P. Yunzheng Pi, M. Ernst and J.-C. Schrotter, Effect of Phosphate Buffer upon CuO/Al2O3 and Cu (II) Catalyzed Ozonation of Oxalic Acid Solution, *Ozone Sci. Eng.*, 2003, **25**, 393.

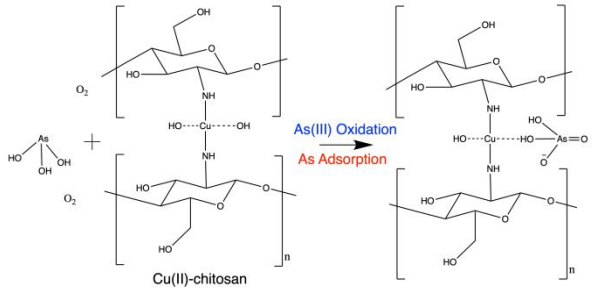

Simultaneous oxidation of As(III) to As(V) and adsorption of As(V) by Cu(II)-chitosan. Arsenic oxidation occurs via a Cu(II)-chitosan catalyzed Fenton-like reaction.